

SCIENTIFIC REPORTS



OPEN

Adenylyl cyclase 3 haploinsufficiency confers susceptibility to diet-induced obesity and insulin resistance in mice

Tao Tong¹, Ying Shen¹, Han-Woong Lee², Rina Yu³ & Taesun Park¹

Received: 25 February 2016
 Accepted: 08 September 2016
 Published: 28 September 2016

Adenylyl cyclase 3 (Adcy3), a member of the mammalian adenylyl cyclase family responsible for generating the second messenger cAMP, has long been known to play an essential role in olfactory signal transduction. Here, we demonstrated that *Adcy3* heterozygous null mice displayed increased visceral adiposity in the absence of hyperphagia and developed abnormal metabolic features characterized by impaired insulin sensitivity, dyslipidemia, and increased plasma levels of proinflammatory cytokines on both chow and high-fat diet (HFD). Of note, HFD decreased the *Adcy3* expression in white adipose tissue, liver, and muscle. We also report for the first time that *Adcy3* haploinsufficiency resulted in reduced expression of genes involved in thermogenesis, fatty acid oxidation, and insulin signaling, with enhanced expression of genes related to adipogenesis in peripheral tissues of mice. In conclusion, these findings suggest that cAMP signals generated by *Adcy3* in peripheral tissues may play a pivotal role in modulating obesity and insulin sensitivity.

Adenylyl cyclases (Adcys), the downstream enzymes for G-protein-coupled receptors (GPCRs), catalyze the conversion of adenosine triphosphate (ATP) into the universal second messenger cyclic AMP (cAMP) which mediates several physiological functions in mammals including embryogenesis, hormone secretion, glycogen breakdown, smooth-muscle relaxation, cardiac contraction, and olfaction^{1–3}. Nine isoforms of membrane-bound Adcys are known, each encoded by a distinct gene. Depending on the properties and the relative levels of the isoforms expressed in a tissue or a cell type at a specific time, extracellular signals received through GPCRs can be integrated differently. In the mammalian brain, mRNA for *Adcy1* and *Adcy2* is highly expressed in regions associated with learning and memory, including the hippocampus, cerebral cortex, and cerebellum¹, while primary cilia of bile cholangiocytes⁴, bone cells⁵, and renal epithelial cells⁶ are known to express *Adcy3*, *Adcy4*, *Adcy6*, and *Adcy8*.

Adcy3 is a 130-kDa glycosylated protein involved in the cascade required for detection of odorants in olfactory neurons⁷. Coupling of odorant receptors to *Adcy3* stimulates cAMP transients that function as the major second messengers for olfactory signaling⁷. *Adcy3* knockout mice (*Adcy3*^{−/−}) are known to be anosmic (unable to smell) and to have a very high fatality rate after birth. It is believed that the neonatal mortality is due to the inability of pups to smell their mother, compromising their ability to nurse⁸. Besides the well-known function of *Adcy3* in regulating olfaction, it has also been suggested to exert ectopic functions based on studies of *Adcy3*-deficient mice^{9–11}. Inactivation of the *Adcy3* gene significantly reduced male fertility: spermatozoa from *Adcy3*^{−/−} male mice exhibited decreased motility and showed an increase in spontaneous acrosome reactions^{9,10}. Moreover, plasma renin and glomerular filtration rates were significantly decreased in *Adcy3*^{−/−} mice, implying that *Adcy3* may play a critical role in regulating fundamental aspects of renal function¹¹.

Several lines of evidence suggest the interesting possibility that *Adcy3* may play an important role in the regulation of adiposity. For example, genetic association studies of the *Adcy3* in Swedish¹² and Chinese¹³ populations led to the discovery of *Adcy3* polymorphisms associated with decreased risk of obesity. Furthermore, Wang *et al.* reported that *Adcy3*^{−/−} mice fed chow exhibited higher total fat mass measured by whole body composition analyzer, hyperphagia, and lower physical activity, and speculated that these phenotypic changes conferred by *Adcy3* knockout were associated with disruption of cAMP signaling in primary cilia of the hypothalamus¹⁴. Pitman

¹Department of Food and Nutrition, Brain Korea 21 PLUS Project, Yonsei University, 50 Yonsei-ro, Seodaemun-gu, Seoul 120-749, South Korea. ²Department of Biochemistry, Yonsei University, 50 Yonsei-ro, Seodaemun-gu, Seoul 120-749, South Korea. ³Department of Food Science and Nutrition, University of Ulsan, Mugeo-dong, Nam-ku, Ulsan 680-749, South Korea. Correspondence and requests for materials should be addressed to T.P. (email: tspark@yonsei.ac.kr)

et al. recently found that the gain-of-function mutation of *Adcy3* gene had increased *Adcy3* activity and cAMP production and consequently the mutant mice had significantly lower total body weights and fat mass compared to wild type controls after 12 weeks of HFD feeding¹⁵. It has been established that cAMP signaling, in addition to its involvement in regulating feeding behavior and leptin sensitivity in the hypothalamus^{16,17}, also has a role in controlling adipose tissue development and function through regulating the expressions of genes related to adipogenesis, lipolysis, and thermogenesis^{18–20}. There is also some evidence to suggest *Adcy3* may play physiological roles in muscle and liver. For example, Griffin *et al.* found that *Adcy3* is expressed in primary muscle cell and is associated with muscle cell migration and adhesion²¹. In addition, hepatic *Adcy3* was reported to play a protective role in insulin resistance and obesity in mice with HFD-induced obesity²². The present study was aimed at determining whether *Adcy3* functions in peripheral tissues related to metabolic disorders by regulating the development of adiposity and insulin resistance in mice.

Results

***Adcy3*^{+/-} mice display increased visceral adiposity.** *Adcy3*^{+/-} mice maintained on HFD for 17 weeks exhibited a significant increase in final body weight (14% for male, $p < 0.05$; 26% for female, $p < 0.01$), cumulative body weight gain (20% for male, $p < 0.05$; 63% for female, $p < 0.05$), and total visceral fat-pad weights (27% for male, $p < 0.05$; 133% for female, $p < 0.01$) as compared to WT mice (Fig. 1a,b,e–g,i). There was no significant difference in food intake between *Adcy3*^{+/-} and WT mice for male and female (Fig. 1c,h). The food efficiency ratio in *Adcy3*^{+/-} mice was significantly higher (16% for male, $p < 0.05$; 100% for female, $p < 0.05$) as compared to WT mice under conditions of HFD feeding (Fig. 1d,i). Male *Adcy3*^{+/-} mice fed chow were found to have significantly higher visceral fat-pad weight as compared to WT mice (Fig. 1e).

Plasma and hepatic biochemical parameters in mice. *Adcy3*^{+/-} mice on HFD exhibited significantly higher levels of plasma TG (29% for male, $p < 0.05$; 26% for female, $p < 0.05$), TC (20% for male, $p < 0.05$; 23% for female, $p < 0.05$), and FFA (27% for male, $p < 0.05$; 26% for female) relative to WT mice (Fig. 2a–c,j–l). Hepatic triglyceride (55% for male, $p < 0.001$; 60% for female, $p < 0.001$), cholesterol (77% for male, $p < 0.001$; 79% for female, $p < 0.001$), and fatty acid (216% for male, $p < 0.001$; 234% for female, $p < 0.001$) levels were significantly higher in *Adcy3*^{+/-} mice relative to levels observed in WT mice on HFD (Fig. 2d–f,m–o). *Adcy3*^{+/-} mice had significantly higher plasma concentrations of leptin (10% for male, $p < 0.05$; 19% for female, $p < 0.05$), IL-6 (16% for male, $p < 0.05$; 23% for female, $p < 0.05$), and TNF α (10% for male, $p < 0.05$; 12% for female, $p < 0.05$) as compared to WT mice on HFD (Fig. 2g–i,p–r). *Adcy3*^{+/-} mice fed chow had significantly higher hepatic triglyceride (23% for male, $p < 0.01$; 25% for female, $p < 0.01$), cholesterol (28% for male, $p < 0.01$; 32% for female, $p < 0.01$), and fatty acid (96% for male, $p < 0.01$; 128% for female, $p < 0.01$) levels than WT mice (Fig. 2d–f,m–o). In the meantime, there was no significant difference in plasma levels of TG, TC, FFA, and proinflammatory cytokines between *Adcy3*^{+/-} and WT mice fed chow irrespective of gender (Fig. 2a–c,g–i,j–l,p–r).

***Adcy3*^{+/-} mice display impaired glucose homeostasis.** The oral glucose tolerance test (OGTT) was performed 2 weeks prior to the end of the experimental period. Integrated plasma glucose concentration, as calculated by area under the curve (AUC), was increased in *Adcy3*^{+/-} mice relative to their WT counterparts on both chow (18% for male, $p < 0.05$; 13% for female) and HFD (26% for male, $p < 0.05$; 32% for female, $p < 0.05$; Fig. 3a,b,f,g). Fasting plasma glucose and insulin levels were measured at the end of the feeding period. *Adcy3*^{+/-} mice fed HFD had significantly higher fasting plasma concentrations of glucose (42% for male, $p < 0.05$; 69% for female, $p < 0.05$; Fig. 3c,h) and insulin (28% for male, $p < 0.05$; 38% for female, $p < 0.05$; Fig. 3d,i) compared with WT mice. Along with the plasma glucose and insulin levels, the HOMA-IR values indicated that insulin sensitivity was significantly decreased in *Adcy3*^{+/-} mice maintained on HFD (Fig. 3e,j).

The protein levels of phosphor-IR, phosphor-IRS1, phosphor-AKT, phosphor-GSK3 β were significantly decreased in the epididymal adipose tissue of *Adcy3*^{+/-} mice relative to WT mice on both chow and HFD (Fig. 4a). The amount of GLUT4 found in the membrane fraction of the epididymal adipose tissue was significantly decreased, whereas the amount of total cellular GLUT4 remained the same in *Adcy3*^{+/-} mice when compared with WT mice (Fig. 4b). Similarly, the protein levels of phosphor-IRS1 and phosphor-AKT were significantly decreased in the liver and muscle of *Adcy3*^{+/-} mice relative to WT mice on both chow and HFD (Fig. 4c,d). The expression of the key gluconeogenesis enzymes, such as *PEPCK* and *G6pase*, were found to be significantly increased in the liver of *Adcy3*^{+/-} mice than in WT mice on both chow and HFD (Fig. 4e).

Insulin-stimulated GLUT4 translocation is decreased in *Adcy3* deficient 3T3-L1 adipocytes. To test whether *Adcy3* affects the insulin-stimulated GLUT4 translocation from cytosol to plasma membrane, we transiently knocked down *Adcy3* using siRNA in 3T3-L1 adipocytes and measured the membrane-bound GLUT4 in the presence of insulin by western blotting. Relative to scrambled siRNA-transfected controls, treatment with siRNA (*Adcy3* SMARTpool) for 48 h achieved significant reductions of *Adcy3* expression level in 3T3-L1 adipocytes (Fig. 4f). The loss of *Adcy3* led to a significant decrease in the amount of plasma membrane GLUT4 after insulin stimulation (Fig. 4g).

***Adcy3* expression in peripheral tissues of mice.** HFD feeding significantly downregulated the mRNA expression of *Adcy1*, *Adcy2*, *Adcy3*, and *Adcy8* in the epididymal adipose tissue of mice but had no effect on the expression of other *Adcy* isoforms (Fig. 5e). *Adcy3*^{+/-} mice showed significantly decreased total *Adcy* activity in the epididymal adipose tissue as compared to WT mice fed chow (–31%, $p < 0.01$) and HFD (–16%, $p < 0.01$) (Fig. 5a). Both mRNA and protein levels of *Adcy3* were significantly reduced in the epididymal adipose tissue of *Adcy3*^{+/-} mice than in WT mice irrespective of diet (Fig. 5b,e). The protein level of *Adcy3* was also significantly decreased in the liver and muscle of *Adcy3*^{+/-} mice relative to WT mice on both chow and HFD. (Fig. 5c,d).

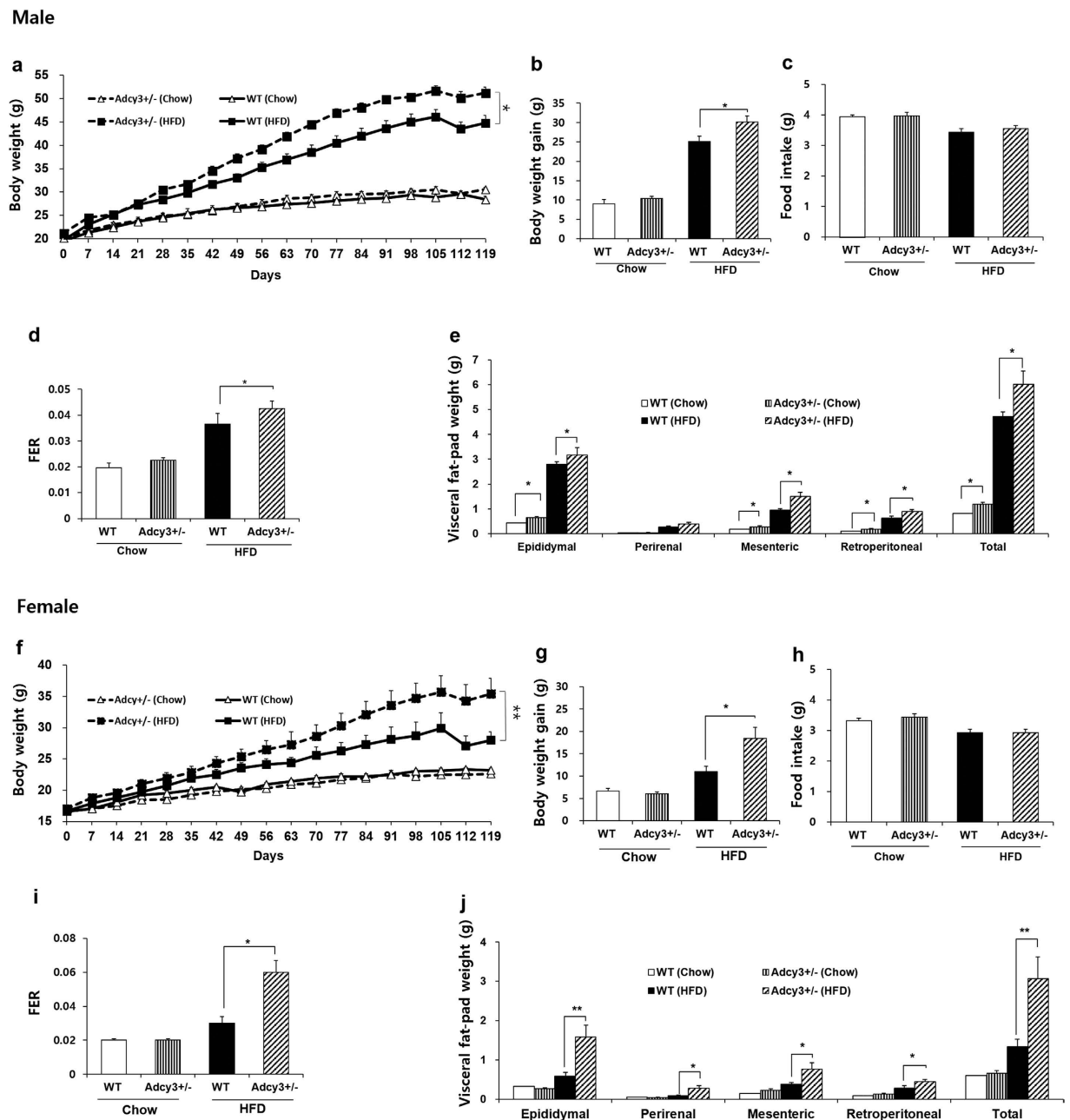


Figure 1. *Adcy3*^{+/-} mice are prone to develop visceral adiposity. (a,f) Changes in body weight during 17 weeks of feeding. (b,g) Cumulative body weight gain. (c,h) Daily food intake. (d,i) Food efficiency ratio (FER; bodyweight gain over the experimental period [g]/food intake over the experimental period [g]). (e,j) Visceral fat-pad weight. Data for both male (upper panels) and female (lower panels) mice are presented. Values are presented as means \pm SEM ($n = 8$). Significant differences between groups are indicated by asterisks; * $P < 0.05$; ** $P < 0.01$; *** $P < 0.001$.

Altered expression of molecules related to adipogenesis, fatty acid oxidation, and thermogenesis in *Adcy3*^{+/-} mice.

The protein levels of PKA, phosphor-AMPK, phosphor-HSL, and phosphor-CREB were found to be significantly lower in the epididymal adipose tissue of *Adcy3*^{+/-} mice than in WT mice on both chow and HFD (Fig. 6b–d). The expression levels of PKA and phosphor-AMPK were also significantly decreased in the liver and muscle of *Adcy3*^{+/-} mice compared with WT mice irrespective of diet (Fig. 6e,f). The expression of genes encoding transcription factors, such as peroxisome proliferator-activated receptor $\gamma 2$ (*PPAR* $\gamma 2$) and CCAAT/enhancer binding protein α (*C/EBP* α), and their targets, adipocyte fatty acid binding protein (*aP2*) and fatty acid synthase (*FAS*), were significantly increased in the epididymal adipose tissue of *Adcy3*^{+/-} mice relative to WT mice on both chow and HFD (Fig. 6a). The mRNA level of carnitine palmitoyl transferase 1 (*CPT1*) were significantly downregulated by *Adcy3* haploinsufficiency in the epididymal adipose tissue of mice on both chow and HFD (Fig. 6h). *Adcy3* haploinsufficiency significantly decreased the expression of thermogenic genes, such as

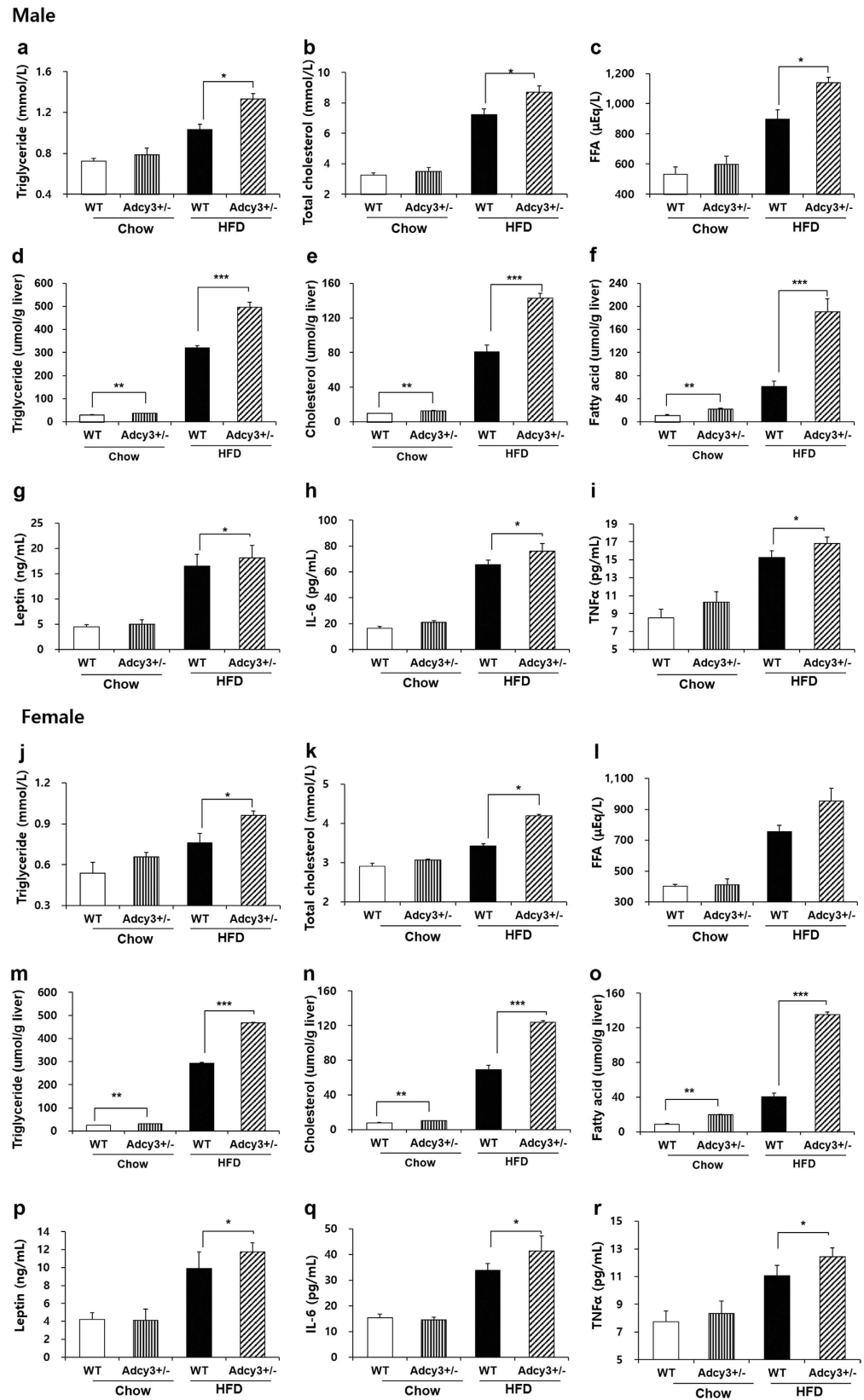


Figure 2. Plasma and hepatic biochemical parameters in mice. Plasma levels of (a,j) triglyceride, (b,k) total cholesterol, and (c,l) FFA. Hepatic contents of (d,m) triglyceride, (e,n) cholesterol, and (f,o) FFA. Plasma levels of (g,p) leptin, (h,q) IL-6, and (i,r) TNF α . Data for both male (upper panels) and female (lower panels) mice are presented. Values are presented as mean \pm SEM ($n = 8$). Significant differences between groups are indicated by asterisks; * $P < 0.05$; ** $P < 0.01$; *** $P < 0.001$.

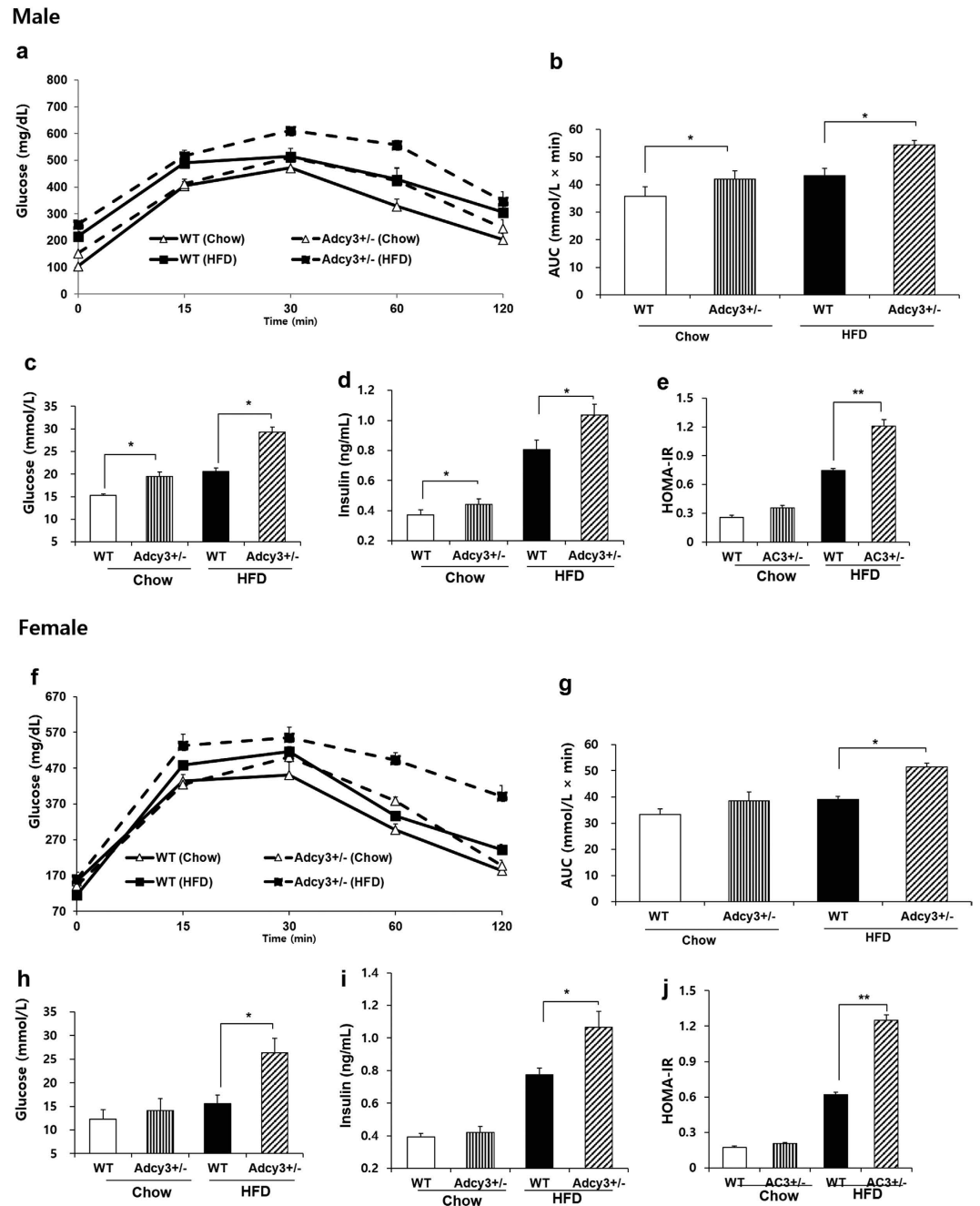


Figure 3. *Adcy3*^{+/-} mice have impaired glucose tolerance and are less insulin sensitive. (a,f) Oral glucose tolerance test. (b,g) Area under the curve. (c,h) Fasting plasma glucose levels. (d,i) Fasting insulin levels. (e,j) Homeostasis model assessment of basal insulin resistance. Data for both male (upper panels) and female (lower panels) mice are presented. Values are presented as means \pm SEM ($n = 8$). Significant differences between groups are indicated by asterisks; * $P < 0.05$; ** $P < 0.01$; *** $P < 0.001$.

peroxisome proliferator-activated receptor gamma co-activator 1-alpha (*PGC1 α*), encoding PR-domain containing 16 (*PRDM16*), uncoupling protein 1 (*UCP1*), T-box transcription factor (*TBX1*), and transmembrane protein 26 (*TMEM26*) in both epididymal and subcutaneous adipose tissues (Fig. 6g,i).

Discussion

Adcy3^{+/-} mice (*Adcy3*^{tm1Dgen/J}) on a 129/OlaHsd background used in the present study were offspring from heterozygous intercross matings of mice originally obtained from the Jackson Laboratory and were found to be healthy and viable. In contrast, homozygous *Adcy3* mice on a 129/OlaHsd background showed a postnatal lethal phenotype²³, and other homozygous *Adcy3* mice on a 129Sv/J background (*Adcy3*^{tm1Drs}) struggled to survive, with an 80% fatality rate within 48 hours, and exhibited abnormal phenotypes, such as anosmia⁸, reduced male fertility¹⁰, and excretory dysfunction of kidney¹¹. In the present study, the increased weight gain and adiposity

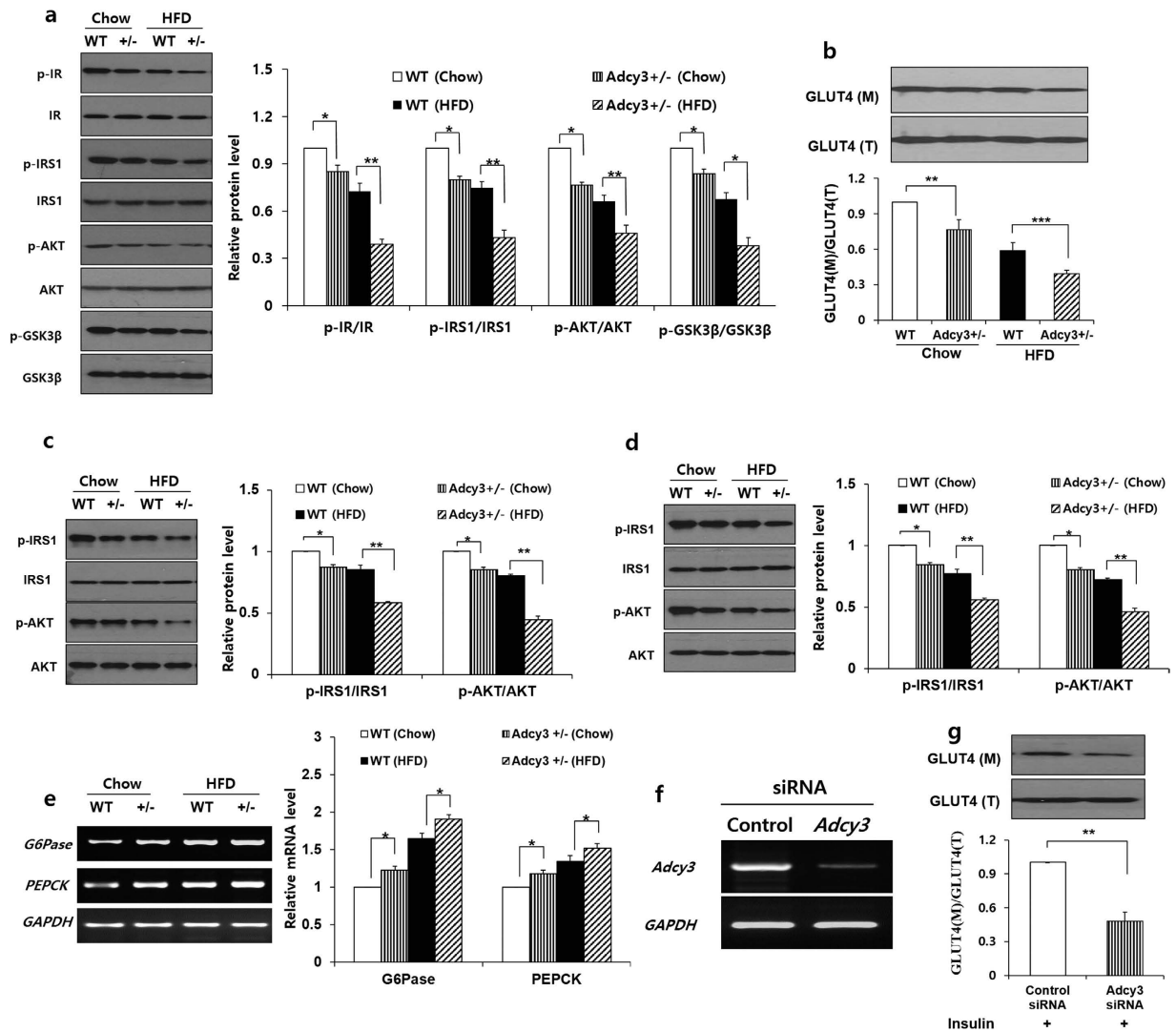


Figure 4. *Adcy3* haploinsufficiency led to impairment of insulin signaling. (a,b) Protein levels of p-IR, IR, p-IRS1, IRS1, p-AKT, AKT, p-GSK3 β , GSK3 β , membrane GLUT4, and total GLUT4 in the epididymal adipose tissue. (c,d) Protein levels of p-IRS1, IRS1, p-AKT, and AKT in the (c) liver and (d) muscle. (e) mRNA levels of *G6Pase* and *PEPCK* in the liver of mice. (f) The knockdown efficiency by siRNA was monitored by semiquantitative RT-PCR. (g) Insulin-stimulated GLUT4 translocation in 3T3-L1 adipocytes treated with control siRNA or siRNA against *Adcy3*. The full-length blots/gels are presented in Supplementary Figs 1–7. Values are presented as means \pm SEM ($n = 8$). Significant differences between groups are indicated by asterisks; * $P < 0.05$; ** $P < 0.01$; *** $P < 0.001$.

observed in the *Adcy3*^{+/-} mice were not associated with the increased consumption of food, thereby suggesting that *Adcy3* haploinsufficiency does not promote hyperphagia. Consistent with our findings, Pitman *et al.* recently revealed that mice carrying a gain-of-function mutation in *Adcy3* (*Adcy3*^{III/+}) were protected from diet-induced obesity due to increased oxygen consumption and physical activity without a change in food intake compared to their WT littermates during the 7 days of whole-body metabolic measurements¹⁵.

In the present study, all membrane-bound *Adcy* isoforms reported, from *Adcy1* through *Adcy9*, were expressed in white adipose tissue (WAT) of mice (Fig. 5). Nevertheless, *Adcy3* appears to be one of the major isoforms contributing to Adcy activity in WAT based on our observation that *Adcy3* haploinsufficiency resulted in a significant decrease (–31%) in total Adcy activity in visceral adipose tissue of mice on chow. Chaudhry *et al.* reported that in brown adipose tissue of rats, the increase in Adcy activity corresponded to a selective upregulation of *Adcy3* expression during the neonatal period when offspring are especially sensitive to environmental conditions and maintenance of body temperature²⁴. Moreover, treatment of neonates with the sympathetic neurotoxin 6-hydroxydopamine abolished the perinatal increase in both Adcy activity and *Adcy3* mRNA levels without affecting the expression of other *Adcy* isoforms²⁴.

In the present study, the HFD-induced decrease in total Adcy activity observed in visceral adipose tissue of both WT and *Adcy3*^{+/-} mice was accompanied by downregulation of *Adcy1*, *Adcy2*, *Adcy3*, and *Adcy8* mRNA expression. This finding is in line with previous reports indicating that expression of *Adcy* isoforms in a specific

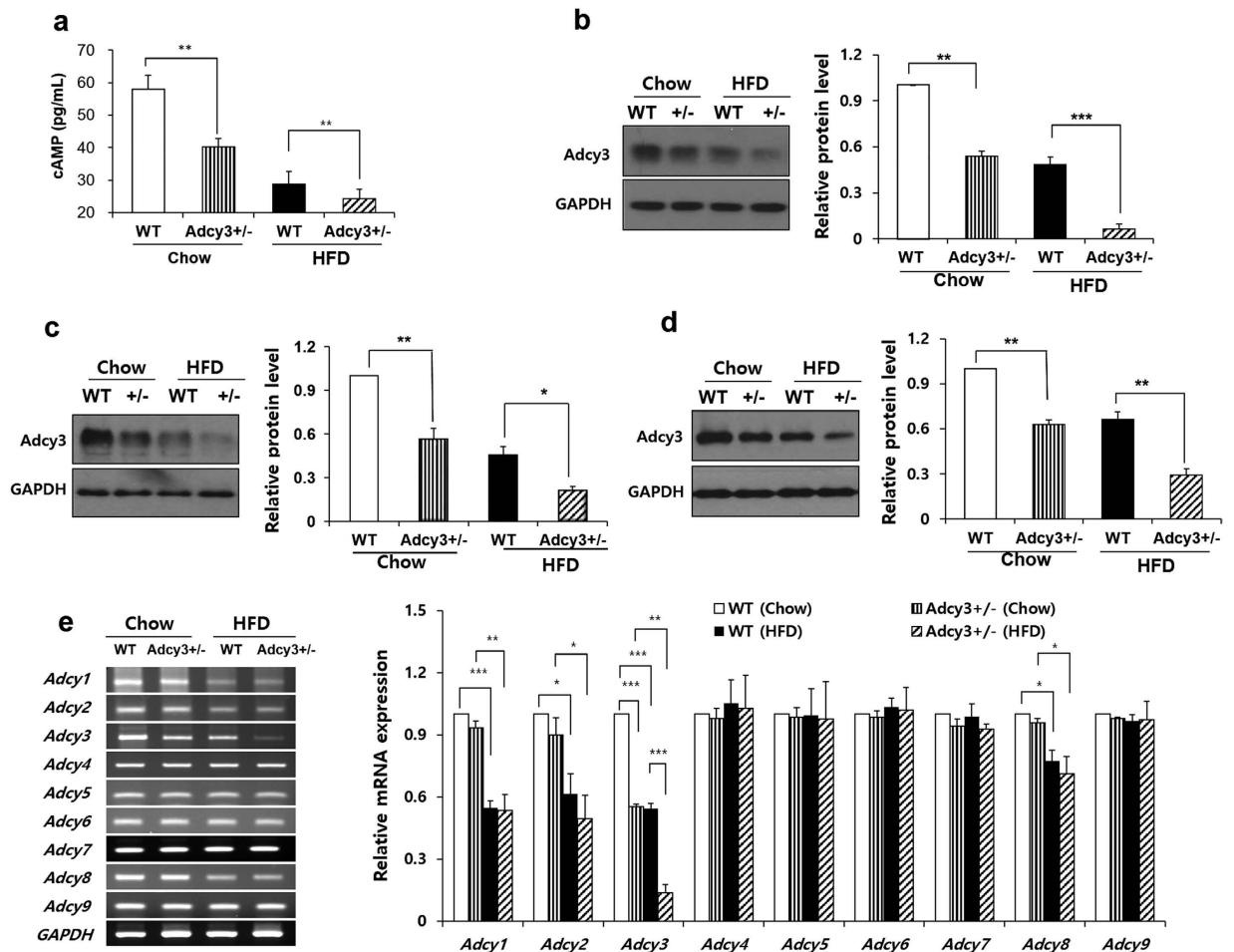


Figure 5. *Adcy3* expression in peripheral tissues of mice. (a) cAMP concentrations in the epididymal adipose tissue of mice. (b–d) Protein level of *Adcy3* in the (b) epididymal adipose tissue, (c) liver, and (d) muscle of mice. (e) mRNA levels of *Adcy* isoforms in the epididymal adipose tissue of mice. The full-length blots/gels are presented in Supplementary Figs 8–11. Values are presented as means \pm SEM ($n = 8$). Significant differences between groups are indicated by asterisks; * $P < 0.05$; ** $P < 0.01$; *** $P < 0.001$.

cell or tissue type can be selectively changed in response to pathophysiologic stimuli^{25,26}. Choi *et al.* observed that treatment of human colon epithelial cells with butyrate, which induced cell differentiation, downregulated mRNA expression of *Adcy3*, *Adcy4*, *Adcy6*, and *Adcy7* by 70–90%, while mRNA levels of the other three isoforms, including *Adcy1*, *Adcy5*, and *Adcy9*, were unchanged²⁵. Furthermore, Suzuki *et al.* reported that among four isoforms of *Adcys* (*Adcy2*, *Adcy6*, *Adcy7*, and *Adcy9*) detected in the gastrocnemius muscle, *Adcy2* and *Adcy9* mRNA were selectively downregulated after denervation carried out by excision of the left sciatic nerve at the midhigh region²⁶.

The cAMP signaling pathways are pivotal in regulation of adipose tissue development and function²⁷. The accumulation of cAMP activates PKA in adipocytes of all colors and origins, thereby phosphorylating several proteins, such as CREB²⁰, AMPK²⁸, and HSL²⁹ (Fig. 7). Phosphor-CREB then activates the expression of PGC-1 α , which induces the transcription of downstream thermogenic genes, including UCP1²⁰. In parallel, phosphorylated AMPK inhibits preadipocyte differentiation by downregulating PPAR γ and C/EBP α , which are the central regulators of adipogenesis and lipid storage in adipocytes³⁰. Moreover, PKA-mediated phosphorylation induces translocation of the HSL to the surface of lipid droplets and enhances its catalytic activity²⁹. The released free fatty acids are oxidized to fatty acyl-CoA which combines with CPT1 to enter mitochondria for its oxidation. In the present study, *Adcy3* haploinsufficiency significantly decreased the protein levels of PKA, phosphor-CREB, phosphor-HSL, and phosphor-AMPK in WAT of mice fed HFD (Fig. 7). These results indicated that in WAT, *Adcy3* might be associated with the regulation of cAMP-PKA-mediated signaling pathways that affect thermogenesis, fatty acid oxidation, and adipogenesis.

Here, *Adcy3* haploinsufficiency reduced insulin sensitivity in mice, as demonstrated by as demonstrated by impairment of insulin signaling in WAT, liver, and muscle, along with increased AUC values and elevated fasting plasma glucose and insulin levels. This insulin resistance observed in *Adcy3*^{+/-} mice appears to be associated with decreased AMPK activity (Fig. 7). Reduced AMPK activity is known to decrease the phosphorylation of IRS-1 at Ser789, thus negatively regulating insulin signaling in adipocytes³¹. Moreover, *Adcy3*^{+/-} mice showed higher

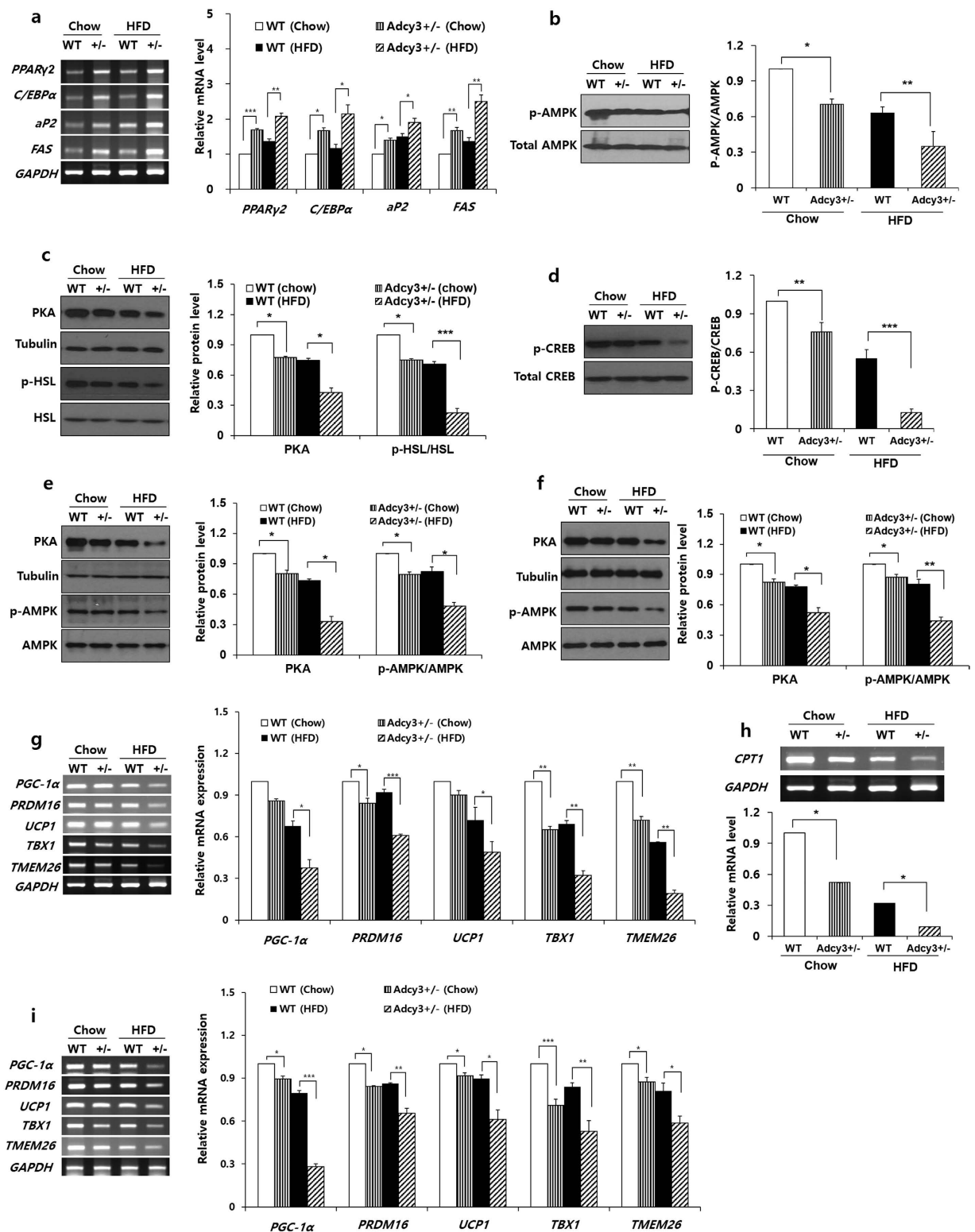


Figure 6. *Adcy3*^{+/-} mice display altered expression of genes related to adipogenesis, fatty acid oxidation, and thermogenesis. (a) mRNA levels of PPAR γ 2, C/EBP α , and their target genes in the epididymal adipose tissues of mice. (b) Protein levels of p-AMPK and total AMPK in the epididymal adipose tissues of mice. (c) Protein levels of PKA, p-HSL, and total HSL in the epididymal adipose tissues of mice. (d) Protein levels of p-CREB and total CREB in the epididymal adipose tissues of mice. (e,f) Protein levels of PKA and p-AMPK in the (e) liver and (f) muscle of mice. (g,h) mRNA levels of thermogenic genes in the (g) epididymal and (h) subcutaneous adipose tissues of mice. (i) Gene expression of CPT1 in the epididymal adipose tissue of mice. The full-length blots/gels are presented in Supplementary Figs 12–20. Values are presented as means \pm SEM ($n = 8$). Significant differences between groups are indicated by asterisks; * $P < 0.05$; ** $P < 0.01$; *** $P < 0.001$.

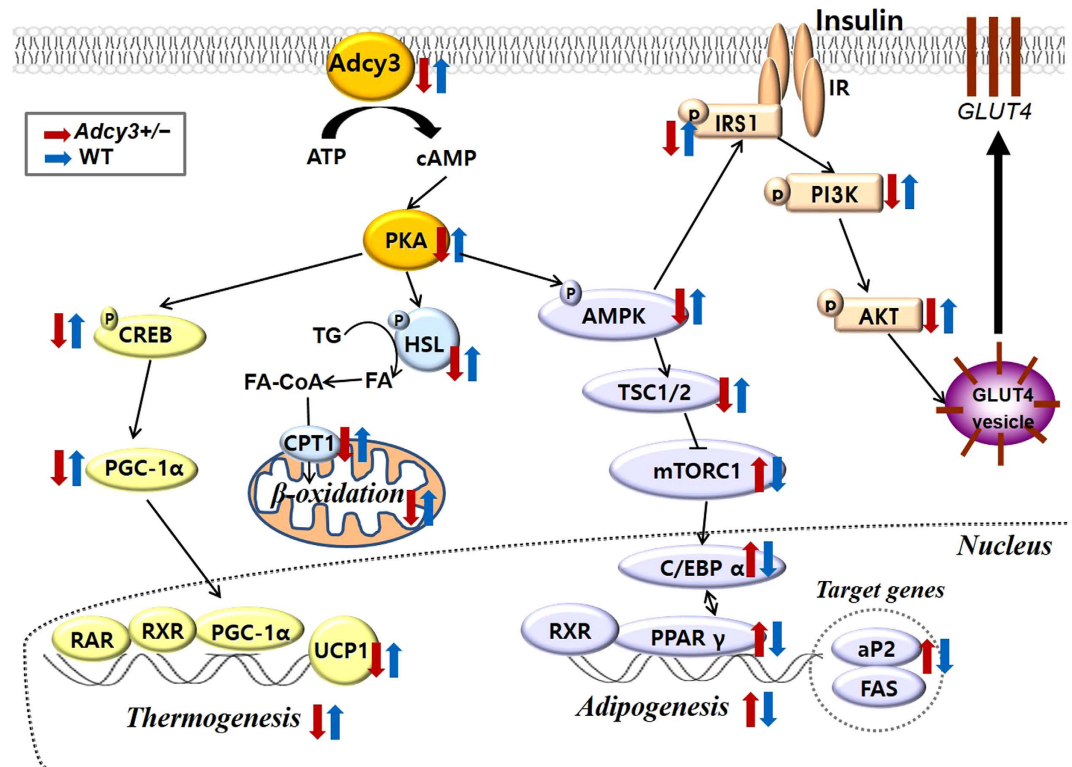


Figure 7. Schematic presentation of the *Adcy3*-mediated signaling pathways related to adipogenesis, thermogenesis, fatty acid oxidation, and insulin resistance.

plasma levels of proinflammatory cytokines, such as IL-6 and TNF α , relative to their WT littermates on both chow and HFD. It is well established that within adipose tissue, IL-6 and TNF α cause adipocyte insulin resistance through inactivation of both the insulin receptor and IRS-1, both of which result in diminished activation of phosphoinositol-3-kinase, the essential second messenger signal that governs most of metabolic effects associated with insulin^{32,33}. Therefore, the increased plasma levels of proinflammatory cytokines could also be a contributing factor for the aggravated insulin resistance in *Adcy3*^{+/-} mice.

Possible application of *Adcy3* as a target for insulin resistance and anti-obesity treatment has been implicated in a recent study by Liang *et al.*²² revealing that hepatic *Adcy3* is upregulated in mice with HFD-induced obesity by liraglutide, a glucagon-like peptide-1 analogue recently approved by the US Food and Drug Administration as an obesity treatment option. In conclusion, the *Adcy3* heterozygous null mice displayed increased visceral adiposity in the absence of hyperphagia and developed abnormal metabolic features on both chow and HFD. We report for the first time that HFD decreased the *Adcy3* expression in white adipose tissue, liver, and muscle and that *Adcy3* haploinsufficiency resulted in reduced expression of genes involved in thermogenesis, fatty acid oxidation, and insulin signaling, with enhanced expression of genes related to adipogenesis in peripheral tissues of mice. Although the role of *Adcy3* in humans has yet to be elucidated, our findings raise the possibility that *Adcy3* activators may be useful agents for the prevention or treatment of obesity and associated metabolic complications.

Methods

Animals and diets. *Adcy3*^{+/-} mice (B6.129P2-*Adcy3*^{tm1Dgen}/J; stock 005773) were generated by Deltagen Inc. (San Mateo, CA, USA) and acquired from the Jackson Laboratories (Bar Harbor, ME, Maine, USA) through the “NIH initiative supporting placement of Deltagen, Inc., mice into public repositories.” Heterozygous intercross was performed to produce *Adcy3*^{+/-} mice and wild-type (WT) littermate control mice. Genotyping was performed using PCR, with genomic DNA extracted from tail tips. Three primers were used: WT (5'-CGT CTT CCT CTA CCT GTG TGC TAT C-3'), mutant (5'-GGG CCA GCT CAT TCC TCC CAC TCA T-3'), and common (5'-TCC TAA CGG ACT TAC ACT GAG GTA G-3').

Four-week-old male and female *Adcy3*^{+/-} or WT littermate mice were housed in a pathogen-free facility at 21 \pm 2.0 $^{\circ}$ C, with 50 \pm 5% relative humidity and a 12-h light/dark cycle. The mice were provided access to rodent chow and tap water *ad libitum* for 1 week. Thereafter, the mice ($n = 8$) were placed on chow or HFD for 17 weeks. The HFD consisted of 200 g fat/kg body weight (170 g of lard and 30 g of corn oil) and 1% (w/w) cholesterol (supplementary Table 1).

Food intake and body weight were measured daily and weekly, respectively. At the end of the experimental period, the mice were anesthetized with diethyl ether after they were fasted for 16 h. Blood samples were drawn from the inferior vena cava into an ethylene-diamine-tetra-acetic acid (EDTA)-coated tube, and the plasma samples were obtained by centrifuging the blood at 4,000 g for 15 min at 4 $^{\circ}$ C. The epididymal,

retroperitoneal, mesenteric, perirenal, and subcutaneous fat-pads were dissected, removed, weighed, and immediately snap-frozen in liquid nitrogen and stored at -80°C until further use. All animal experiments were performed in accordance with the Korea Food and Drug Administration guidelines. All experimental protocols were reviewed and approved by the Institutional Animal Care and Use Committee of the Yonsei Laboratory Animal Research Center (Permit no. 2011-0062).

Cell culture and transfection. 3T3-L1 fibroblasts obtained from American Type Culture Collection (Manassas, VA, USA) were grown in Dulbecco's modified Eagle's medium supplemented with 10% fetal bovine serum, penicillin (50 units/mL), and streptomycin (50 mg/mL). The cells were grown at 37°C in a humidified 5% CO_2 atmosphere. We treated confluent cultures with 0.5 mM 3-isobutyl-1-methylxanthine, 0.25 mM dexamethasone, and 10 mg/mL insulin to promote the differentiation of 3T3-L1 cells into adipocytes. After 2 days, the 3-isobutyl-1-methylxanthine and dexamethasone were removed, and insulin was continued for another 2 days. The growth medium was replenished at 2-day intervals until adipocyte differentiation. For *Adcy3* knock-down, the differentiated adipocytes were treated with 50 nM of either control siRNA (nontargeting SMARTpool, catalog no. D-001810-10-05, Dharmacon, Lafayette, CO, USA) or siRNA against *Adcy3* (On-TARGET plus SMART pool siRNA, catalog no. L-0588903-00-10, Dharmacon) on the ninth day of differentiation. Two days post-transfection, serum-starved cells were treated with 17 nM insulin for 15 min and then lysed for RNA or protein. The knockdown efficiency by siRNA was monitored by semiquantitative RT-PCR.

Biochemical analysis. Plasma content of total cholesterol (TC), triglyceride (TG), free fatty acid (FFA), and glucose were enzymatically determined using individual commercial kits (Bio-Clinical System, Gyeonggi-do, South Korea). Plasma concentration of insulin was measured using a commercially available mouse enzyme-linked immunosorbent assay (ELISA) kit (Millipore, Billerica, MA, USA). The homeostasis model assessment of basal insulin resistance (HOMA-IR) was calculated as [fasting plasma glucose \times fasting plasma insulin/22.5] to assess insulin resistance. Hepatic lipids were extracted as described using the method developed by Folch *et al.*³⁴. Triglyceride, cholesterol, and FFA levels in the hepatic lipid extracts were measured using the same enzymatic kits that were used for the plasma analyses.

Oral glucose tolerance test. The OGTT was performed 2 weeks before the end of the experimental period on 6 h-fasted mice by oral glucose administration (gavage with 2 g glucose/kg body weight). Blood glucose was measured from tail blood at times 0, 15, 30, 60, 90, and 120 min after glucose administration.

Western blotting analysis. To obtain total protein, the liver, muscle, and epididymal and subcutaneous adipose tissue samples obtained from each mouse were homogenized at 4°C in an extraction buffer containing 100 mmol/L Tris-HCl (pH 7.4), 5 mmol/L EDTA, 50 mmol/L NaCl, 50 mmol/L sodium pyrophosphate, 50 mmol/L NaF, 100 mmol/L orthovanadate, 1% Triton X-100, 1 mmol/L phenylmethanesulfonyl fluoride, 2 $\mu\text{g}/\text{mL}$ aprotinin, 1 $\mu\text{g}/\text{mL}$ pepstatin A, and 1 $\mu\text{g}/\text{mL}$ leupeptin, and centrifuged at 13,000 g for 20 min at 4°C . To obtain membrane protein, the epididymal and subcutaneous adipose tissue samples were homogenized in a buffer containing 20 mmol/L HEPES (pH 7.4), 4 mmol/L EDTA, 250 mmol/L sucrose, two tablets of protein inhibitor, 1 mmol/L sodium orthovanadate, and 1% Triton X-100. The homogenates were centrifuged at 2,000 g for 1.5 h at 4°C , and the supernatant fractions were centrifuged at 150,000 g for 1.5 h at 4°C . Protein concentrations were measured by Bradford assay (Bio-Rad, Hercules, CA, USA).

Total protein or membrane protein (40 μg) was separated by 8% sodium dodecyl sulfate (SDS)-polyacrylamide gel electrophoresis (PAGE) and then electrophoretically transferred to nitrocellulose membranes (Amersham, Buckinghamshire, UK). The nitrocellulose membranes were incubated overnight with primary antibodies (diluted 1:1,000) at 4°C . Antibodies to the following proteins were commercially obtained from the indicated sources: β -actin and *Adcy3* from Santa Cruz Biotechnology (Santa Cruz, CA, USA) and AMP-activated protein kinase (AMPK), phosphor-AMPK (Thr172), cyclic AMP-responsive element-binding protein (CREB), phosphor-CREB (Ser133), PKA, hormone-sensitive lipase (HSL), phosphor-HSL (Ser563), insulin receptor β subunit (IR β), phosphor-IR β (Tyr1162/1163), insulin receptor substrate 1 (IRS1), phosphor-IRS1 (Ser789), protein kinase B (AKT), phosphor-AKT (Ser473), glycogen synthase kinase-3 β (GSK3 β), phosphor-GSK3 β (Ser9), and glucose transporter type 4 (GLUT4) from Cell Signaling Technology (Danvers, MA, USA). Secondary antibodies were applied for 1 hr at room temperature in Tris-buffered saline containing 0.05% Tween-20. Signal was detected by using a chemiluminescent detection system (Amersham). The protein bands were quantified using Quantity One Analysis Software (Bio-Rad).

Adcy enzymatic assay. Fifty microliters of Adcy mixture [100 mM Tris-acetate (pH 7.4), 20 mM KCl, 10 mM MgCl_2 , 20 mM phosphoenolpyruvate, 100 $\mu\text{g}/\text{mg}$ pyruvate kinase, 2 mM ATP, 20 μM guanosine triphosphate, 2 mM dithiothreitol, 0.4 mM bovine serum albumin, and 0.1 mM 3-isobutyl-1-methylxanthine] and 125 μg of membrane fractions from epididymal adipose tissue were added into microcentrifugation tubes in duplicate and maintained at 4°C . The reaction tubes were incubated in a water bath maintained at 37°C for 30 min, and the reaction was terminated by heating at 95°C for 5 min. The supernatant solution was stored after centrifugation at 10,000 g for 5 min at 4°C . The cAMP assay was performed using the cAMP ELISA kit from Enzo Life Sciences International, Inc. (Plymouth Meeting, PA, USA).

RNA extraction and semi-quantitative reverse transcriptase-polymerase chain reaction (RT-PCR). Total RNA was isolated from the liver, epididymal, and subcutaneous adipose tissue of each mouse by using TRIzol (Invitrogen, Carlsbad, CA, USA) and was reverse-transcribed by using the Superscript II Kit (Invitrogen) according to the manufacturer instructions. The PCR was programmed as follows: 10 min at 94°C ,

30–35 cycles of 94 °C for 30 s, 55 °C for 30 s, 72 °C for 1 min, and 10-min incubation at 72 °C. Then, 5 µL of each PCR product was mixed with 1 µL of 6-fold concentrated loading buffer and electrophoresed on a 2% agarose gel containing ethidium bromide. The band intensities were quantified using the Quantity One Analysis Software (Bio-Rad). The mRNA levels were normalized to that of the glyceraldehyde-3-phosphate dehydrogenase transcript. Sequences of all primers are listed in supplementary Table 2.

Statistics. Results on body weight gain and plasma biochemistries are presented as the mean \pm standard error of mean (SEM) of eight mice in each group. The RT-PCR and western blot data are shown as the means \pm SEM of three independent experiments ($n = 2$ or 3 per experiment) for each group, cumulatively including eight mice. An unpaired Student *t*-test analysis was used for all data comparisons between the *Adcy3*^{+/-} and WT control mice fed chow or HFD. All statistical analyses were performed with SPSS 21.0 software (IBM, Corp., Armonk, NY, USA), and significance was set at **P* < 0.05, ***P* < 0.01 and ****P* < 0.001.

References

- Hanoune, J. & Defer, N. Regulation and role of adenylyl cyclase isoforms. *Annu. Rev. Pharmacol.* **41**, 145–174 (2001).
- Cooper, D. M. Regulation and organization of adenylyl cyclases and cAMP. *Biochem. J.* **375**, 517–529 (2003).
- Seed Ahmed, M. *et al.* Increased expression of adenylyl cyclase 3 in pancreatic islets and central nervous system of diabetic Goto-Kakizaki rats: a possible regulatory role in glucose homeostasis. *Islets* **4**, 343–348 (2012).
- Masyuk, A. I. *et al.* Cholangiocyte primary cilia are chemosensory organelles that detect biliary nucleotides via P2Y(12) purinergic receptors. *Am. J. Physiol-Gastr. L.* **295**, G725–G734 (2008).
- Kwon, R. Y., Temiyasathit, S., Tummala, P., Quah, C. C. & Jacobs, C. R. Primary cilium-dependent mechanosensing is mediated by adenylyl cyclase 6 and cyclic AMP in bone cells. *Faseb. J.* **24**, 2859–2868 (2010).
- Raychowdhury, M. K. *et al.* Vasopressin receptor-mediated functional signaling pathway in primary cilia of renal epithelial cells. *Am. J. Physiol-Renal* **296**, F87–F97 (2009).
- Wang, H. & Storm, D. R. Calmodulin-regulated adenylyl cyclases: cross-talk and plasticity in the central nervous system. *Mol. Pharmacol.* **63**, 463–468 (2003).
- Wong, S. T. *et al.* Disruption of the type III adenylyl cyclase gene leads to peripheral and behavioral anosmia in transgenic mice. *Neuron* **27**, 487–497 (2000).
- Gautier-Courteille, C., Salanova, M. & Conti, M. The olfactory adenylyl cyclase III is expressed in rat germ cells during spermiogenesis. *Endocrinology* **139**, 2588–2599 (1998).
- Livera, G. *et al.* Inactivation of the mouse adenylyl cyclase 3 gene disrupts male fertility and spermatozoon function. *Mol. Endocrinol.* **19**, 1277–1290 (2005).
- Pluznick, J. L. *et al.* Functional expression of the olfactory signaling system in the kidney. *Proc. Natl. Acad. Sci. USA* **106**, 2059–2064 (2009).
- Nordman, S. *et al.* Genetic variation of the adenylyl cyclase 3 (AC3) locus and its influence on type 2 diabetes and obesity susceptibility in Swedish men. *Int. J. Obesity* **32**, 407–412 (2008).
- Wang, H. R. *et al.* Evaluation of the association between the AC3 genetic polymorphisms and obesity in a Chinese Han population. *PLoS One* **5**, e13851 (2010).
- Wang, Z. *et al.* Adult type 3 adenylyl cyclase-deficient mice are obese. *PLoS One* **4**, e6979 (2009).
- Pitman, J. L. *et al.* A gain-of-function mutation in adenylyl cyclase 3 protects mice from diet-induced obesity. *PLoS One* **9**, e110226 (2014).
- Zhao, A. Z. Control of food intake through regulation of cAMP. *Curr. Top. Dev. Biol.* **67**, 207–224 (2005).
- Zhao, A. Z., Huan, J. N., Gupta, S., Pal, R. & Sahu, A. A phosphatidylinositol 3-kinase phosphodiesterase 3B-cyclic AMP pathway in hypothalamic action of leptin on feeding. *Nat. Neurosci.* **5**, 727–728 (2002).
- Rogne, M. & Tasken, K. Compartmentalization of cAMP signaling in adipogenesis, lipogenesis, and lipolysis. *Horm. Metab. Res.* **46**, 833–840 (2014).
- Carmen, G. Y. & Victor, S. M. Signalling mechanisms regulating lipolysis. *Cell. Signal.* **18**, 401–408 (2006).
- Cao, W. H. *et al.* p38 mitogen-activated protein kinase is the central regulator of cyclic AMP-dependent transcription of the brown fat uncoupling protein 1 gene. *Mol. Cell. Biol.* **24**, 3057–3067 (2004).
- Griffin, C. A., Kafadar, K. A. & Pavlath, G. K. MOR23 Promotes Muscle Regeneration and Regulates Cell Adhesion and Migration. *Dev. Cell* **17**, 649–661 (2009).
- Liang, Y. *et al.* Hepatic adenylyl cyclase 3 is upregulated by Liraglutide and subsequently plays a protective role in insulin resistance and obesity. *Nutr. Diabetes* **6**, e191 (2016).
- Deltagen Inc. NIH initiative supporting placement of Deltagen, Inc. mice into public repositories. *MGI Direct Data Submission*, <http://www.informatics.jax.org/reference/j:101679> (2005).
- Chaudhry, A., Muffler, L. A., Yao, R. H. & Granneman, J. G. Perinatal expression of adenylyl cyclase subtypes in rat brown adipose tissue. *Am. J. Physiol-Reg. I.* **270**, R755–R760 (1996).
- Choi, L. J. *et al.* Coordinate down-regulation of adenylyl cyclase isoforms and the stimulatory G protein (G(s)) in intestinal epithelial cell differentiation. *J. Biol. Chem.* **285**, 12504–12511 (2010).
- Suzuki, Y. *et al.* Expression of adenylyl cyclase mRNAs in the denervated and in the developing mouse skeletal muscle. *Am. J. Physiol-Cell Ph.* **274**, C1674–C1685 (1998).
- Madsen, L. & Kristiansen, K. The importance of dietary modulation of cAMP and insulin signaling in adipose tissue and the development of obesity. *Ann. N. Y. Acad. Sci.* **1190**, 1–14 (2010).
- Yin, W., Mu, J. & Birnbaum, M. J. Role of AMP-activated protein kinase in cyclic AMP-dependent lipolysis in 3T3-L1 adipocytes. *J. Biol. Chem.* **278**, 43074–43080 (2003).
- Djouder, N. *et al.* PKA phosphorylates and inactivates AMPK alpha to promote efficient lipolysis. *Embo. J.* **29**, 469–481 (2010).
- Habinowski, S. A. & Witters, L. A. The effects of AICAR on adipocyte differentiation of 3T3-L1 cells. *Biochem. Bioph. Res. Co.* **286**, 852–856 (2001).
- Liu, Q. Q., Gauthier, M. S., Sun, L., Ruderman, N. & Lodish, H. Activation of AMP-activated protein kinase signaling pathway by adiponectin and insulin in mouse adipocytes: requirement of acyl-CoA synthetases FATP1 and Acs11 and association with an elevation in AMP/ATP ratio. *Faseb. J.* **24**, 4229–4239 (2010).
- Rotter, V., Nagaev, I. & Smith, U. Interleukin-6 (IL-6) induces insulin resistance in 3T3-L1 adipocytes and is, like IL-8 and tumor necrosis factor-alpha, overexpressed in human fat cells from insulin-resistant subjects. *J. Biol. Chem.* **278**, 45777–45784 (2003).
- Olefsky, J. M. & Glass, C. K. Macrophages, inflammation, and insulin Resistance. *Annu. Rev. Physiol.* **72**, 219–246 (2010).
- Folch, J., Lees, M. & Sloane Stanley, G. H. A simple method for the isolation and purification of total lipides from animal tissues. *J. Biol. Chem.* **226**, 497–509 (1957).

Acknowledgements

This research was supported by Technology Commercialization Support Program (Program no. 1130373), Ministry of Agriculture, Food and Rural Affairs, and SRC program (Center for Food & Nutritional Genomics: Grant no. 2015R1A5A6001906) of the National Research Foundation of Korea funded by the Ministry of Education, Science, and Technology.

Author Contributions

T.T., Y.S. and T.P. designed the experiments, researched and analyzed data, and wrote the manuscript. H.W.L. and R.Y. contributed to experimental design and reviewed and edited the manuscript.

Additional Information

Supplementary information accompanies this paper at <http://www.nature.com/srep>

Competing financial interests: The authors declare no competing financial interests.

How to cite this article: Tong, T. *et al.* *Adenylyl cyclase 3* haploinsufficiency confers susceptibility to diet-induced obesity and insulin resistance in mice. *Sci. Rep.* **6**, 34179; doi: 10.1038/srep34179 (2016).



This work is licensed under a Creative Commons Attribution 4.0 International License. The images or other third party material in this article are included in the article's Creative Commons license, unless indicated otherwise in the credit line; if the material is not included under the Creative Commons license, users will need to obtain permission from the license holder to reproduce the material. To view a copy of this license, visit <http://creativecommons.org/licenses/by/4.0/>

© The Author(s) 2016